Proton Transport

DOI: 10.1002/ange.201105118

High Proton Conductivity of Water Channels in a Highly Ordered Nanowire**

*H. Wang, X. Xu, N. M. Johnson, N. K. R. Dandala, and H.-F. Ji**

We report a highly conductive material for protons based on a crystalline nanoassembly of trimesic acid and melamine (TMA·M). The nanoassembly is prepared by evaporation of water in TMA·M solutions. Because of the highly ordered structure of the nanoassembly, the water-saturated proton conductivity for the TMA·M nanoassembly is 5.5 $S\,cm^{-1}$, which is the highest proton-conductive material to date. This exceptionally high conductivity and low-cost fabrication of the material may make practical applications feasible for fuel cell devices.

For over a century we have been able to directly convert chemical energy into electrical power.[1] The fuel cells responsible for this phenomenon have been shown to be a highly promising, clean alternative to the traditional energy sources in use today.[2] Their use outside of niche applications, however, has been held back by the lack of appropriate and cost-effective materials, including those used for the transport of protons. Much research has consequently been conducted on this topic and has resulted in a wide variety of advanced materials, from polymers to salts,[3,4] all of which are compared to Nafion, the industry standard in terms of costs and conductivity. The conductivity of a bulk Nafion film is 0.1 $S\,cm^{-1}$, and material costs for the ionomer are around $100 per kilogram, ignoring the cost of processing the membrane.[5] A material with a higher conductivity and lower overall associated costs could make the fuel cell technology more competitive.

To be proton-conductive a material must have protons to conduct and it must have a means to transport them. Much research has been conducted on the addition of proton carriers to existing materials, mainly by the addition of acidic groups.[3,6,7] Recently, it has been discovered that ordered nanostructures are capable of improving the proton transfer of proton-conductive materials. This can work by providing a more ordered pathway for existing proton transfer, such as aligning ionomers in an electrospun polymer,[8,9] by improving the mobility of proton carriers, such as incorporating imidazole into nanochannels,[10] or even by creating a structure through which proton transfer can occur where none existed before, such as introducing water to well-structured coordination polymers.[11] This can increase the conductivity by as much as an order of magnitude,[9] illustrating the importance of structure in facilitating conductivity. By combining these two methods and creating a highly ordered structure which includes available protons, such as those in acidic groups, it is expected that materials with extremely high proton conductivities can be created.

Highly ordered supramolecular structures with protons available for transfer can be readily created from self-assembling organic molecules through hydrogen bonds and other interactions.[12,13] One example is a widely studied system built from melamine (M) derivatives and various organic acids,[14–17] which are formed from hierarchical stacking of 2D hydrogen-bonding networks. The low-cost materials and the simple self-assembling processes are added advantages in the applications of these supramolecular structures.

However, although the study of highly ordered self-assembled structures has been fruitful and yielded a wide variety of supramolecular systems,[18] these supramolecular systems have been largely neglected in the field of fuel cells,[19,20] which may be partially due to most of these systems being molecular assemblies,[21] but not assemblies at nano-, micro- or even larger scales. Here we report the formation of crystalline nanowires of melamine with trimesic acid (TMA) (Figure 1) by means of a common solvent evaporation approach and their proton-conductive characteristics. Proton conductivity greater than the highest reported value for the industry standard of Nafion was observed in the ordered nanowires of melamine and TMA. The high conductivity combined with the use of inexpensive reagents and an exceedingly simple synthetic process, makes this structure promising as a future material for industrial fuel cells.

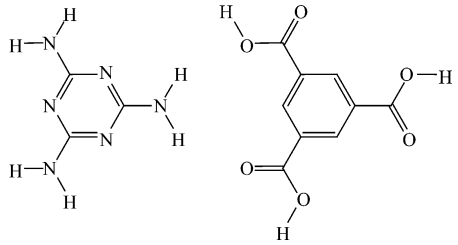

Figure 1. Molecular structures of melamine and trimesic acid.

The nanowires of trimesic acid and melamine were crystallized from water (see the Supporting Information). Figure 2 shows scanning electron microscopy (SEM) images of nanowires of melamine/TMA complexes. These wires have a diameter of 100–400 nm and a length up to 30 μm. The

[*] H. Wang, X. Xu, N. M. Johnson, N. K. R. Dandala, H.-F. Ji
Department of Chemistry, Drexel University
3141 Chestnut St, Philadelphia, PA 19104 (USA)
E-mail: hj56@drexel.edu

[**] H.J. thanks for support from the National Institutes of Health (grant number 1R01NS057366) and the National Natural Science Foundation of China (grant number 20728506/B05).

Supporting information for this article is available on the WWW under http://dx.doi.org/10.1002/anie.201105118.

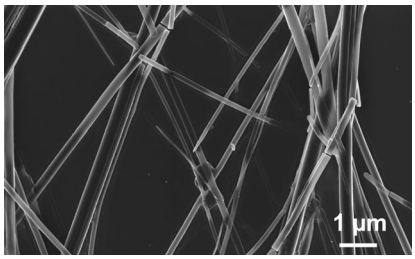

Figure 2. SEM images of 1:1 trimesic acid/melamine.

diameter of the wires can grow to more than 10 μm if all the solvent is evaporated. Once formed, these wires are very stable in water. They do not disintegrate after being stored in water for months.

Figure 3 shows the conductivity of a single TMA·M nanowire in anhydrous and humid environments at 25 °C. The nanowire shows a semiconductive property in anhydrous N_2 (Figure 3 A) and an electrolyte conductive property (Figure 3 B, linear *I–V* curve) at a relative humidity (RH) of 100 % at 25 °C. Furthermore, the conductivity increases 10^6 times when the RH increases from 50 % to 100 %. These results indicate that the conductivity originates from electron transportation in anhydrous environment, and proton conduction dominates in high RH environment. The conductivity change is reversible between low- and high-humidity environments and the process can last more than hundreds of switches without significant signal deviation, suggesting that the structure of the nanowires does not change with different RH values. The maximum conductivity of TMA·M nanowires in 100 % RH is 5.5 $S\,cm^{-1}$. This conductivity shows that the TMA·M nanowire is the most proton-conductive material to date. Table 1 shows the conductivity at different temperatures. The temperature dependence of the proton conductivity (Figure 3 C) shows the Arrhenius plots of proton conductivity of a TMA·M nanowire. The activation energy (E_a) of the TMA·M nanowire was found to be 0.12 eV, which is the lowest E_a in materials for proton conduction, including the industry standard of Nafion ($E_a = 0.22$ eV). It is also lower than E_a for inorganic materials, such as $H_3PMo_{12}O_{40}\cdot 29\,H_2O$ ($E_a = 0.15$ eV),[22] $Sb_2O_5\cdot 4\,H_2O$ ($E_a = 0.17$ eV),[23] and β-$Al_{10.34}Mg_{0.66}O_{17}(H_3O)_{1.66}$ ($E_a = 0.17$ eV).[24] It is close to the 0.11 eV of 1 M HCl solution.

Table 1: Relationship between conductivity and temperature of a TMA·M nanowire.

Temperature [°C]	30	40	50	60	70
Conductivity [$S\,cm^{-1}$]	5.51	6.90	11.0	12.3	18.9

To understand the high proton-conductive property of the TMA·M nanowires, we characterized the nanowires with thermal analysis, transmission electron micrsocpy (TEM), and X-ray crystal diffraction. The thermal properties of the TMA·M nanowires are shown in Figure 4, with comparison to that of TMA and melamine individually. The weight losses of melamine and TMA occur at 250 and 300 °C, respectively. Three weight losses were observed in the thermalgravimetric analysis of TMA·M nanowires. The first weight loss occurs near 100 °C, which can be attributed to the release of water. The weight loss of water is approximately 14.11 %, which corresponds to three water molecules for each TMA ($M_w = 210\,g\,mol^{-1}$) or melamine ($M_w = 126\,g\,mol^{-1}$). The remaining two weight losses occur at 250 and 300 °C, corresponding to the stepwise loss of melamine and TMA, respectively. The weight losses of melamine and TMA are 28.5 and 48.4 %, indicating that the molar ratio of melamine and TMA is 1:1. The final ratio of TMA, melamine, and water in the nanowires

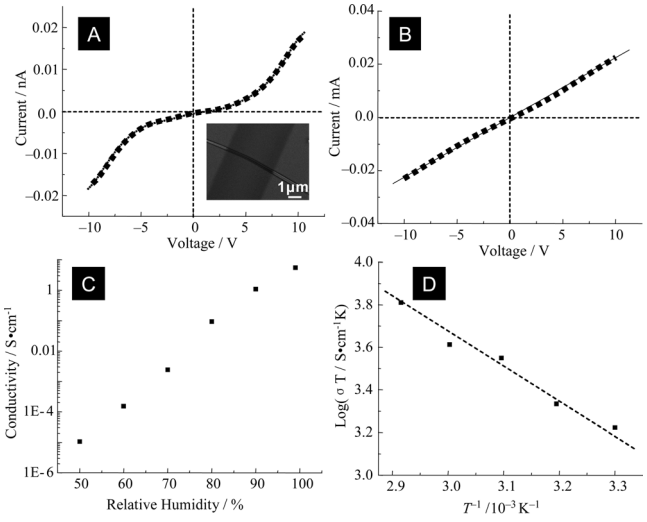

Figure 3. a) *I–V* curve of a single TA·M nanowire measured in anhydrous nitrogen. The inset shows a SEM image of a single TMA·M nanowire bridging two gold elecrodes. The Au electrodes were deposited on both sides of the nanowire by thermal evaporation through a photolithography process. b) *I–V* curve of a single TMA·M nanowire measured at a relative humidity of 100 % at 25 °C. c) Humidity-dependent proton conductivity (25 °C) of a single TMA·M nanowire. d) Arrhenius plot of the proton conductivity (σ) of a single TMA·M nanowire at a relative humidity of 100 %. The single TMA·M nanowire was placed between two gold electrodes for conductivity measurements.

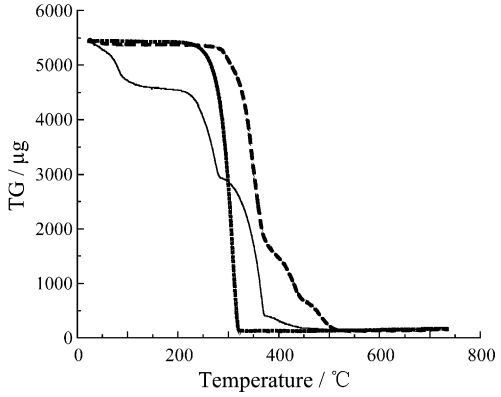

Figure 4. Thermalgravimetric analysis of trimesic acid (-----), melamine (•••••), and TMA·M (——) complex in 1:1 ratio.

is therefore 1:1:3, which is consistent with that obtained from the TMA·M crystal reported by Zhang et al.[25]

TEM images show that the nanowires of TMA·M have a crystalline structure (Figure 5). The corresponding electron diffraction pattern (Figure 5 inset) shows 3.63 Å *d* spacing in the longitudinal nanowire direction, which suggests that the

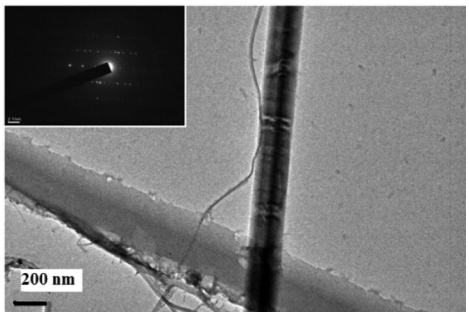

Figure 5. TEM image and electron diffraction of a TMA·M wire.

molecules are oriented with their π–π stacking direction parallel to the wire, as shown in Figure 6. X-ray diffraction shows that the TMA·M nanowire is crystalline and the lattice indices are $a = 6.93$ Å, $b = 11.27$ Å, and $c = 11.68$ Å, indicating a triclinic structure of the microwires, which is the same as those plate crystals obtained in organic–aqueous binary solvents.[25] The TEM and crystal data shows that there are highly ordered water channels inside the nanowires and the direction of the channels is parallel to the direction of the nanowire (Figure 6). In each channel, there are four water molecules on one layer followed by two water molecules in the next layer, and these layers alternate along the channel. This is consistent with the 1:1:3 ratios discussed above. Each water molecule is interconnected through hydrogen bonding with two neighboring ones in different layers into helical chains. Each channel contains a pair of 1:1 left- and right-handed helices along the direction of the nanowires. Each TMA molecule provides one free proton and hydrogen atoms in the other two carboxylic acids are involved in hydrogen bonding with water or melamine in the layer. Every two adjacent layers are bridged through hydrogen bonding of water–water, water–melamine, water–TMA, and J-type aggregation. The layers have a brickwork type of arrangement as shown in Figure 6. No hydrogen bonding of melamine–melamine, TMA–TMA, and TMA–melamine between two adjacent layers was observed.

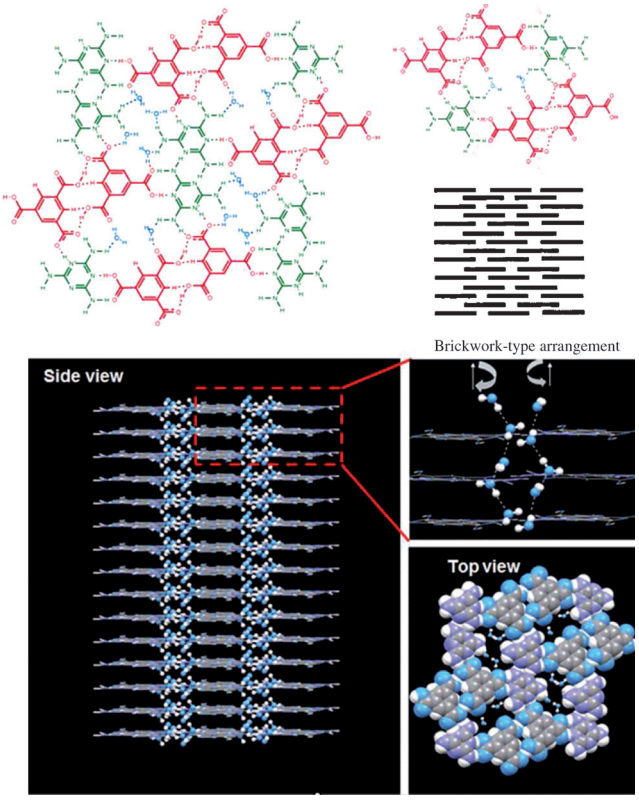

Figure 6. Different views of the hydrogen-bonding network: Top) One layer, two layers, and a brickwork-type arrangement of the molecular structure of the nanowire. Bottom) Top and side view of a space-filling model to show included water molecules and the stacking of layers and two water channels. The water channels are parallel to the direction of the nanowire.

The high proton conductivity could be attributed to highly ordered helical water chains residing in the pores of the 1D crystal structure,[21] which can then efficiently transfer the numerous available protons of the acid–base complex along the axis of the nanowire. When the activation energy is in the range of 0.1–0.4 eV, proton transfer can generally be attributed to the Grotthuss mechanism,[26,27] which describes proton transport of excess protons through reforming hydrogen bonds between H_3O^+ ions and water molecules. The low activation energy of the system (0.12 eV) corresponds approximately to the cleavage of a hydrogen bond, indicating that proton transfer proceeds through a Grotthuss mechanism. Similar ordered water chains can be seen in other structures, and have been shown to allow for facile proton conduction.[28,29]

Distilled water was used in both nanowire preparation and conductivity tests. Trace amount of acids will significantly increase the conductivity. For instance, the conductivity of the nanowire increased more than one order of magnitude when the nanowire is exposed to 1M HCl vapor. The chemistry related to this phenomenon will be further studied in the future.

In summary, we have developed a crystalline TMA·M nanowire that is highly proton conductive by crystallization from water. The proton conductivity at room temperature is 5.5 $S\,cm^{-1}$, which is greater than known proton-conductive materials. This high conductivity can be attributed to the highly ordered water helix in the pores of the wire. The extensive hydrogen bonding provides an excess of protons for transport, which can then proceed along the axis of the wire through the water helix via a Grotthuss hopping mechanism, as indicated by the low activation energy of the system.

Currently, we are investigating approaches to tackle the challenge of placing the nanocrystals in an ordered arrangement between the cathode and the anode of fuel cells before the nanowires can be practically used for fuel cell applications. Future work in this area also includes further improve-

ment of the conductivity under low-humidity and high-temperature conditions, which is critical for practical applications of automotive fuel cells,[30,31] by growing the nanowires in porous membranes or by using other aromatic carboxylic acids or aromatic sulfonic acids to provide more free protons. Growing nanowires in ordered, porous membranes, such as anodized Al_2O_3, will not only secure the fast transportation of protons in the anticipated direction between a cathode and an anode, but also enhance the robustness of the nanowires.

Overall, this discovery may expand the search for highly proton-conductive materials among the large and versatile family of self-assembled supramolecular complexes, and the facile and controllable synthesis method makes it competitive for the creation of proton-conductive materials, which may have wide applications.

Received: July 21, 2011
Revised: October 12, 2011
Published online: November 3, 2011

Keywords: fuel cells · hydrogen bonds · proton transport · self-assembly · water channels

[1] W. R. Grove, *Philosoph. Mag. J. Sci.* **1842**, *21*, 417 – 420.
[2] W. Vielstich, H. A. Gasteiger, H. Yokokawa, *Handbook of fuel cells: advances in electrocatalysis, materials, diagnostics and durability*, *Vol. 6*, Hoboken, Wiley, **2009**.
[3] J. Peron, Z. Shi, S. Holdcroft, *Energy Environ. Sci.* **2011**, *4*, 1575 – 1591.
[4] S. M. Haile, D. A. Boysen, C. R. I. Chisholm, R. B. Merle, *Nature* **2001**, *410*, 910 – 913.
[5] M. Gebert, B. Holhlein, D. Stolten, *J. Fuel Cell Sci. Technol.* **2004**, *1*, 56 – 60.
[6] C. Chow, *J. Mater. Chem.* **2010**, *20*, 6245 – 6249.
[7] J. C. McKeen, Y. S. Yan, M. E. Davis, *Chem. Mater.* **2008**, *20*, 3791 – 3793.
[8] T. Tamura, H. Kawakami, *Nano Lett.* **2010**, *10*, 1324 – 1328.
[9] B. Dong, L. Gwee, D. S. Cruz, K. I. Winey, Y. A. Elabd, *Nano Lett.* **2010**, *10*, 3785 – 3790.
[10] S. Bureekaew, S. Horike, M. Higuchi, M. Mizuno, T. Kawamura, D. Tanaka, N. Yanai, S. Kitagawa, *Nat. Mater.* **2009**, *8*, 831 – 836.
[11] T. Yamada, M. Sadakiyo, H. Kitagawa, *J. Am. Chem. Soc.* **2009**, *131*, 3144 – 3145.
[12] S. C. Zimmerman, F. Zeng, D. F. C. Reichert, C. V. Kolotuchin, *Science* **1996**, *271*, 1095 – 1098.
[13] A. P. H. J. Schenning, E. W. Meijer, *Chem. Commun.* **2005**, 3245 – 3258.
[14] G. M. Whitesides, J. P. Mathias, C. T. Seto, *Science* **1991**, *254*, 1312 – 1319.
[15] J. P. Mathias, E. E. Simanek, J. A. Zerkowski, C. T. Seto, G. M. Whitesides, *J. Am. Chem. Soc.* **1994**, *116*, 4316 – 4325.
[16] X. Sun, H. T. Jonkman, F. Silly, *Nanotechnology* **2010**, *21*, 165602.
[17] H. Walch, A. Maier, W. M. Heckl, M. Lackinger, *J. Phys. Chem. C* **2009**, *113*, 1014 – 1019.
[18] F. J. M. Hoeben, P. Jonkheijm, E. W. Meijer, A. P. H. Schenning, *Chem. Rev.* **2005**, *105*, 1491 – 1546.
[19] Y. Chen, M. Thorn, S. Christensen, C. Versek, A. Poe, R. C. Hayward, M. T. Tuominen, S. Thayumanavan, *Nat. Chem.* **2010**, *2*, 503 – 508.
[20] J. Ding, C. Chuy, S. Holdcroft, *Chem. Mater.* **2001**, *13*, 2231 – 2233.
[21] G. V. Oshovsky, D. N. Reinhoudt, W. Verboom, *Angew. Chem.* **2007**, *119*, 2418 – 2445; *Angew. Chem. Int. Ed.* **2007**, *46*, 2366 – 2393.
[22] O. Nakamura, T. Kodama, J. Ogino, Y. Migake, *Chem. Lett.* **1979**, 17 – 18.
[23] W. A. England, M. G. Cross, A. Hamnett, P. J. Wiseman, J. B. Goodenough, *Solid State Ionics* **1980**, *1*, 231 – 249.
[24] N. Baffier, J. C. Badot, P. Colomban, *Solid State Ionics* **1984**, *13*, 233 – 236.
[25] X. L. Zhang, X. M. Chen, *Cryst. Growth Des.* **2005**, *5*, 617 – 622.
[26] P. Colomban, A. Novak, *J. Mol. Struct.* **1988**, *177*, 277 – 308.
[27] N. Agmon, *Chem. Phys. Lett.* **1995**, *244*, 456 – 462.
[28] A. Mukherjee, M. K. Saha, M. Nethaji, A. R. Chakravarty, *Chem. Commun.* **2004**, 716 – 717.
[29] J. M. Taylor, R. K. Mah, I. L. Moudrakovski, C. I. Ratcliffe, R. Vaidhyanathan, G. K. H. Shimizu, *J. Am. Chem. Soc.* **2010**, *132*, 14055 – 14057.
[30] S. M. Haile, D. A. Boysen, C. R. I. Chisholm, R. B. Merle, *Nature* **2001**, *410*, 910 – 013.
[31] M. Ide, H. Ikeda, *J. Renewable Sustainable Energy* **2009**, *1*, 043102.

